oxidative DNA damage, lipid peroxidation and micronuclei formation, and increases hydrogen peroxide and nitric oxide production in BEAS-2B cells, a human bronchial epithelial cell line, but anTiO$_2$ 200 nm particles do not (Gurr et al., 2005). In contrast, both nano-sized and 200nm ruTiO$_2$ are toxic *in vitro* (Gurr et al., 2005; Sayes et al., 2006). On the other hand, under ultraviolet irradiation, anTiO$_2$ is 100 times more toxic to human dermal fibroblasts and A549 cells than rnTiO$_2$, and is more potent than rnTiO$_2$ in the induction of lactate dehydrogenase release, reactive oxygen species production and interleukin 8 secretion (Sayes et al., 2006). Experimental data demonstrating differences in the toxic effects of anTiO$_2$ and rnTiO$_2$ *in vivo*, however, are still lacking.

Respiratory exposure to nTiO$_2$ particles can occur both at the workplace, e.g., in manufacturing and packing sites, and outside the workplace during their use (Maynard et al., 2006; Schulte et al., 2008). In the present study, we delivered anTiO$_2$ and rnTiO$_2$ to the rat lung by trans-tracheal intra-pulmonary spraying (TIPS) and compared lung inflammation and several toxicological parameters induced by anTiO$_2$ and rnTiO$_2$. The results indicated that obvious lung inflammatory lesions were not observed in the rats, and anTiO$_2$ or rnTiO$_2$ particles were phagocytosed by alveolar macrophages. Analysis of alveolar macrophage induction, 8-OHdG level in the lung, and MIP1α expression both *in vivo* in the lung and *in vitro* in PAM indicated that anTiO$_2$ elicited lower levels of biological responses than rnTiO$_2$. Long-term toxic effects of anTiO$_2$ and rnTiO$_2$ still need to be clarified.

Materials and Methods

Preparation and characterization of nTiO$_2$ suspension

Nanosized TiO$_2$ particles (anatase type without coating, primary size 25 nm and rutile type without coating, primary size 20 nm) were provided by Japan Cosmetic Association, Tokyo, Japan. Both anTiO$_2$ and rnTiO$_2$ particles were suspended in saline at 500 μg/ml and then autoclaved. The suspensions were sonicated for 20 min shortly before use to prevent aggregate formation.

Characterization of nTiO$_2$ was conducted as follows: The shapes of nTiO$_2$ in suspension were imaged by transmission electron microscopy (TEM) and scanning electron microscopy (SEM). Element analysis was performed by a an X-ray microanalyzer (EDAX, Tokyo, Japan), after aliquots of nTiO$_2$ were loaded onto a carbon sheet. For size distribution analysis, aliquots of the 500 μg/ml nTiO$_2$ suspension were loaded onto clean glass slides and photographed under a polarized light microscope (Olympus BX51N-31P-O polarized light microscope, Tokyo, Japan), and the photos were then analyzed by an image analyzer system (IPAP, Sumika Technos Corporation, Osaka, Japan). Over 1000 particles of anTiO$_2$ and rnTiO$_2$ were measured.

Animals

Female Sprague-Dawley rats (SD rats) were purchased from CLEA Japan Co., Ltd (Tokyo, Japan). The animals were housed in the animal center of Nagoya City University Medical School, maintained on a 12 hour light-dark cycle and received oriental MF basal diet (Oriental Yeast Co., Tokyo, Japan) and water *ad lib*. The research was conducted according to the Guidelines for the Care and Use of Laboratory Animals of Nagoya City University Medical School and the experimental protocol was approved by the Institutional Animal Care and Use Committee (H22M-19).

Trans-tracheal intra-pulmonary spraying (TIPS) protocol

Three groups of 6 female SD rats (Group 1, saline; Group 2, anTiO$_2$; and Group 3, rnTiO$_2$) aged 9 weeks were acclimated for 7 days prior to the start of the study. Saline and nTiO$_2$ suspensions were administered by TIPS to the animals under isoflurane anesthesia: The nozzle of a Microsprayer (series IA-1B Intratracheal Aerosolizer, Penn-century, Philadelphia, PA) connected to a 1 ml syringe was inserted into the trachea through the larynx and a total volume of 0.5 ml suspension was sprayed into the lungs synchronizing with spontaneous inspiration by the animal (Xu et al., 2010). Rats were treated once every the other day over a 2 week period, a total of eight treatments. The total amount of anTiO$_2$and rnTiO$_2$ administered to Groups 2 and 3 was 2.0 mg per rat. Six hours after the last spraying, the animals were killed and the whole lung was excised and divided into two parts; the left lung was cut into pieces and immediately frozen at -80°C and used for biochemical analysis, and the right lung was fixed in 4% paraformaldehyde solution in phosphate-buffered saline (PBS) adjusted to pH 7.3 and processed for immunohistochemical, light microscopic and transmission electron microscopic (TEM) examinations.

Light microscopy and transmission electron microscopy

Hematoxylin and eosin (H&E) stained sections were used for pathological observation. The number of alveolar macrophages in H&E lung tissue slides was counted and expressed as number per mm^2.

Slides were observed under light microscopic observation, the corresponding area in the paraffin block was cut out, deparaffinized and embedded in epoxy resin and processed for TEM and titanium element analysis with a JEM-1010 transmission electron microscope (JEOL Co. Ltd, Tokyo, Japan) equipped with an X-ray microanalyzer (EDAX, Tokyo, Japan).

Analysis of 8-hydroxydeoxy guanosine levels

For the analysis of 8-hydroxydeoxyguanosine (8-OHdG) levels, genomic DNA was isolated from a piece of the left lung with a DNA Extractor WB kit (Wako Chemicals Co. Ltd). 8-OHdG levels were determined with an 8-OHdG ELISA Check kit (Japan Institute for Control of Aging, Shizuoka, Japan).

RNA isolation, cDNA synthesis and RT-PCR analysis of gene expression

Pieces of the left lungs (50-100 mg) were thawed, rinsed 3 times with ice cold PBS, and total RNA was isolated using 1 ml Trizol Reagent (Invitrogen, Karlsruhe, Germany). For reverse transcription PCR (RT-PCR) and real-time PCR, first strand cDNA synthesis from 2 mg of total RNA was performed using SuperScript™ III First-Strand Synthesis

System (Invitrogen of Life Technologies, CA) according to the manufacturer's instructions. PCR primers for rat MIP1α were 5'-TTTTGAGACCAGCAGCCTTT -3' (forward) and 5'- CTCAAGCCCCTGCTCTACAC-3' (reverse), and the product size was 191bp. b-actin was used as internal control and the primers were 5'- AGCCATGTACGTAGCCATCC-3' (forward) and 5'-CTCTCAGCTGTGGTGGTGAA-3', and the product size was 228 bp. RT-PCR was conducted using an iCycler (BioRad Life Sciences, CA) as follows: 95°C 20 sec, 60°C 20 sec, 72°C 30sec, 30 cycles for MIP1α; and 95°C 20 sec, 60°C 20 sec, 72°C 30sec, 15 cycles for b-actin. Real-time PCR analysis of MIP1α gene expression was performed with a 7300 Real Time PCR System (Applied Biosystem, CA) using Power SYBR Green PCR Master Mix (Applied Biosystem, CA) according to the manufacturer's instructions. b-actin gene was used as the normalizing reference gene.

Immunohistochemical analysis

Paraffin embedded lung tissues sections were immunostained with polyclonal anti-rat MIP1α (BioVision, Lyon, France). Antigen retrieval was carried out by microwave for 20 min in 10 mmol/L citrate buffer (pH 6.0). Antibody was diluted 1:100 in blocking solution and applied to the slides, and the slides were incubated at 4°C overnight. Immunohistochemical staining was done by the avidin-biotin complex method (ABC) using the Vectastain Elite ABC system (Vector Laboratories, Burlingame, CA). Biotinylated goat anti-rabbit IgG (Vector Laboratories) was used as a secondary antibody at a dilution of 1:500 for 1 hour and visualized using avidin-conjugated alkaline phosphatase complex (ABC kit, Vector laboratories) and Alkaline Phosphatase Substrate Kit (Vector Laboratories). Sections were lightly counterstained with hematoxylin for microscopic examination.

ELISA for MIP1α in the lung tissues and the supernatants of cell culture

Left lung tissue samples (50-100mg) were thawed, rinsed 3 times with ice cold PBS and homogenized in 1 ml of tissue extraction reagent (PeproTech, London, UK) containing 1% (v/v) Proteinase Inhibitor Cocktail (Sigma-Aldrich, St Louis, MO, USA). The homogenates were clarified by centrifugation at 10,000g, 4°C for 5 min. The protein content in the supernatants was measured with a BCATM Protein assay kit (Pierce). The levels of MIP1α in the supernatants were measured using rat MIP1α ELISA Development Kit (Cat#: 900-K75, Peprotech, Inc., Rocky Hill, NJ.) according to the manufacturer's instruction, and expressed as pg/mg lung tissue protein. The levels of MIP1α in cell culture supernatants were measured as described above and expressed as pg/ml.

Isolation of PAM and exposure of $nTiO_2$ to PAM cells

Induction and isolation of alveolar macrophages in female SD rats was performed as described previously (Xu et al., 2010). 10^6 primary alveolar macrophages (PAM) were cultured in RPMI1640 containing 2% fetal bovine serum and antibiotics overnight at 37°C, 5% CO_2. 500 μg/ml of $anTiO_2$ and $rnTiO_2$ suspensions was then added to the cultures to a final concentration of 10 μg/ml and the cells were incubated for another 24 hours. RNA was isolated from the PAM and the level of MIP1α protein in the conditioned culture media was measured by ELISA.

In vitro cell proliferation assay

A549 cells were seeded into 96-well culture plates at 2×10^3 cells per well in 2% fetal bovine serum Dulbecco's modified Eagle's medium (Wako Chemicals Co., Ltd). After overnight incubation, the medium was replaced with the conditioned PAM culture media treated with $anTiO_2$ or $rnTiO_2$, and the cells were incubated for another 72 hours, with or without 20 μg/ml of anti-MIP1α neutralizing antibody (R&D Systems, Minneapolis, MN). The relative cell number of A549 cells was determined using a Cell counting Kit-8 (Dojindo Molecular Technologies, Rockville, MD) according to the manufacturer's instruction.

Cytotoxicity assay in vitro

A549 cells, the primary human lung fibroblast cell line CCD34 (ECACC, Cat. No. 90110514) and PAM were used for cytotoxicity analyses. Cells were seeded in 96 well plates at 5×10^3/well and incubated overnight. The cells were then treated with $anTiO_2$ and $rnTiO_2$ suspensions at final concentrations of 0, 2, 10, or 50 μg/ml and then incubated for another 24 hours. The relative cell number was determined as described above.

Cytotoxicity of $anTiO_2$ and $rnTiO_2$ under ultraviolet B irradiation

A549 cells were used for analysis of $nTiO_2$ cytotoxicity under ultraviolet irradiation. First, we determined an irradiation time that did not affect the cell viability as follows: A549 cells were seeded into 96 well plates at 1×10^3/well in 200 μL Dulbecco's modified Eagle's medium (Wako Chemicals Co., Ltd) containing 10% fetal bovine serum and incubated overnight. The cells were irradiated with ultraviolet B (UVB) for 0, 30 sec, 1 min, 2 min, 5 min and 10 min with a transilluminator (Vilber Lourmat, France). The light intensity was 1000 mW/cm^2, and the emission spectrum was from 270 nm to 330 nm with a peak at 312 nm. The non-irradiated control wells were covered with a sterile aluminium sheet to prevent irradiation. The relative cell number was determined after incubation for 48 hours at 37°C, 5% CO_2.

Next, we observed the effect of $anTiO_2$ and $rnTiO_2$ on cell viability under UVB. A549 cells were seeded into 96 well plate at 1×10^3well in 100 μL culture media and incubated overnight. Then, 100 mL of $anTiO_2$ or $rnTiO_2$ suspensions in DMEM culture medium containing 10% FBS was added into the wells to final concentration of 0, 2, 5 and 10 μg/ml and incubated for 30 min. The cells were irradiated with UVB for 2 min (2 min UVB irradiation did not affect cell viability), and incubated for another 48 hours, before determination of relative cell number.

Statistical and analysis

Statistical significance of the *in vitro* and *in vivo* findings was analyzed using the two-tailed Student's t-test. *In vitro* and *in vivo* data are presented as means±standard

deviations. A value of $p<0.05$ was considered to be significant.

Results

Characterization of $nTiO_2$ particles in suspension

TEM images showed that individual $anTiO_2$ particles were spherical in shape, while individual $rnTiO_2$ particles had a rod-like shape, and both $anTiO_2$ and $rnTiO_2$ formed large aggregates in suspension (Figure. 1A and B). Similarly, SEM observation indicated aggregate formation of both types of $nTiO_2$ particles (Figure. 1C and D). Peaks of titanium (green arrows) and oxygen (blue arrows), which are present in both types of $nTiO_2$ particles, and carbon (white arrows) and nitrogen (red arrow), which are present in the carbon sheets used in the SEM, were observed by elemental scanning (Figure. 1E and F). Peaks of other elements were not detected in either the $rnTiO_2$ or $anTiO_2$ samples. Analyses of particle size showed that the mean and medium diameters were 5.491±2.727 mm and 5.127 mm for $anTiO_2$, and 3.799±2.231 mm and 3.491 mm for $rnTiO_2$ (Figure. 1G), confirming aggregate formation of both types of $nTiO_2$ particles in suspension.

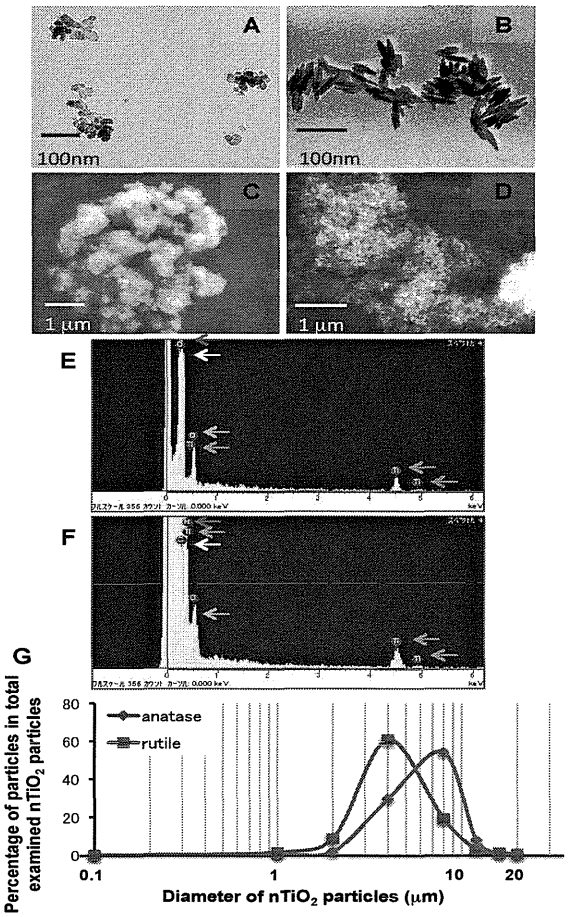

Figure 1. Characterization of $nTiO_2$ Particles in Suspension. A and B: TEM imagines of $anTiO_2$ and $rnTiO_2$ particles in suspension. C and D: SEM images of $anTiO_2$ and $rnTiO_2$ particles. E and F: Element scanning showed peaks of titanium (green arrows), oxygen (blue arrows), carbon (white arrows) and nitrogen (red arrows) in $anTiO_2$ and $rnTiO_2$ particles. G: Size distribution of $anTiO_2$ and $rnTiO_2$ in suspension

Histological observation and 8-OHdG level in the lung tissue

Only a few small lung inflammatory lesions were observed in rats treated with $anTiO_2$ and $rnTiO_2$ (Figure. 2A, B and C). Alveolar macrophage infiltration was found throughout the lung tissue, and most of the alveolar macrophages were seen with phagocytosed $anTiO_2$ particles or $rnTiO_2$ particles (Figure. 2D, E an F). TEM observation demonstrated that both $anTiO_2$ and $rnTiO_2$ were deposited in various sizes in the cytoplasm of the alveolar macrophages (Figure. 2G and H). Neither $anTiO_2$ or $rnTiO_2$ particles were found in other types of cells in the lung tissue. The number of macrophages per mm^2 lung tissue section was 67.1±15.8 (saline), 165.0±34.9 ($anTiO_2$) and 214.2±44.1 ($rnTiO_2$). The numbers of macrophages in the $anTiO_2$ and $rnTiO_2$ treated groups was significantly higher than in the control group ($p<0.001$), and the $anTiO_2$ treated group had lower macrophage infiltration than the $rnTiO_2$ treated group.

The level of 8-OHdG, a parameter of oxidative DNA damage caused by reactive oxygen species (ROS), in the lung tissue in rats treated with $anTiO_2$ and $rnTiO_2$ was 1.96±0.77 and 3.07±1.25 (pg per mg DNA), respectively, and was higher than that of the control (1.44±0.63): The increase in 8-OHdG in the lungs of $rnTiO_2$, but not $anTiO_2$, treated rats was significantly higher than the control

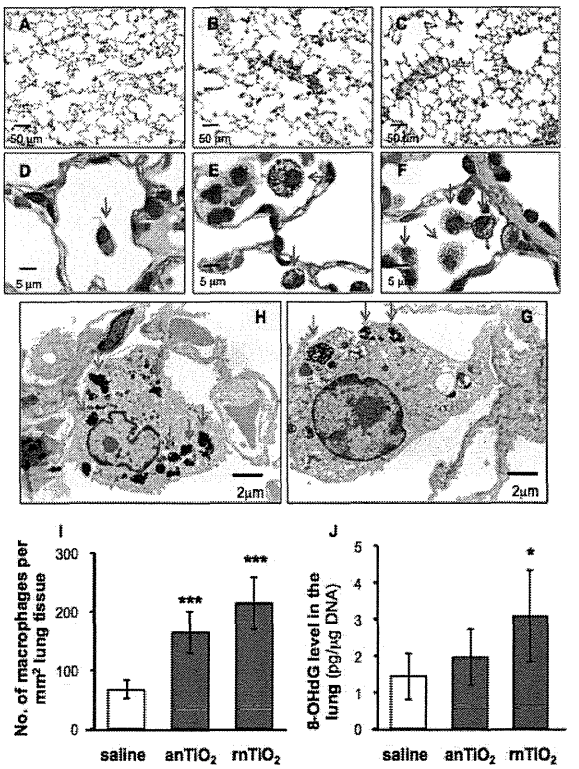

Figure 2. Histological Observation and 8-OHdG Level in the Lung Tissue. A, B and C: Histological imagines of lung tissue treated with saline, $anTiO_2$ and $rnTiO_2$, respectively. Green arrows indicate small inflammatory lesions. D (saline), E ($anTiO_2$) and F ($rnTiO_2$): Higher magnification imagines of alveolar macrophages (brown arrows). $nTiO_2$ particles are clearly observed. G and H: TEM imagines of alveolar macrophages with $anTiO_2$ and $rnTiO_2$ particles in their cytoplasm (blue arrows). I and J: The numbers of alveolar macrophages and 8-OHdG levels in the lung tissue. *, *** represent $p<0.05$ and 0.001, respectively, versus saline

($p<0.05$) (Figure. 2J).

MIP1α expression in the lung tissue

RT-PCR suggested an increase in MIP1α mRNA expression in lung tissue treated with $anTiO_2$ or $rnTiO_2$ (Figure. 3A). Real-time PCR analysis indicated that compared with the control group, the increase was 2.79-fold for $anTiO_2$ and 5.35-fold for $rnTiO_2$. MIP1α mRNA expression was also significantly lower in the $anTiO_2$ treated group compared to the $rnTiO_2$ treated group (Figure. 3B). The levels of MIP1α protein in the lung tissue were 32.8±0.31 and 52.7±0.58 pg/mg lung protein in the $anTiO_2$ and $rnTiO_2$ treated groups, both significantly higher than that of the control group (20.8±0.24) (Figure. 3C). Similarly to MIP1α mRNA expression, MIP1α protein expression was significantly lower in the $anTiO_2$ treated group compared to the $rnTiO_2$ treated group.

To find out what cells in the lung accounted for the increased MIP1α protein expression, we examined tissue samples using MIP1α immunohistochemistry. As shown in Figure. 3D, E and F, MIP1α protein was produced by $anTiO_2$ or $anTiO_2$ burdened alveolar macrophages.

Exposure of PAMs to $anTiO_2$ and $rnTiO_2$ and cell proliferation assays in vitro

As in the lung tissue, *in vitro* exposure of PAM to $nTiO_2$ induced expression of MIP1α mRNA (Figure. 4A) and protein (Figure. 4B). Treatment with $anTiO_2$ and $rnTiO_2$ caused 11.96-fold and 15.26-fold increases in the expression of MIP1α mRNA, respectively, in cultured PAM. The level of MIP1α protein in the cell culture medium was 32.8±1.1 pg/mL for $anTiO_2$ and 52.7±1.3 pg/mL for $rnTiO_2$, significantly higher than that of the control

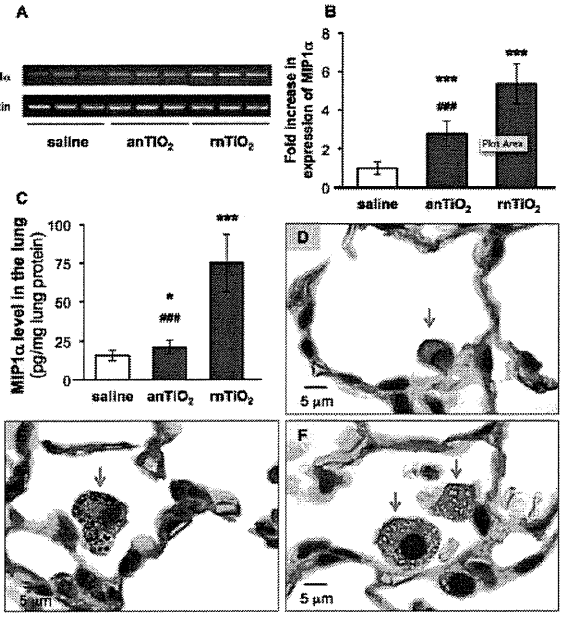

Figure 3. Expression of MIP1α in the Lung Tissue. A, B and C: Analysis of expression of MIP1α mRNA by RT-PCR (A) and real-time PCR (B) and protein by ELISA (C). D, E, and F: Immunohistochemistry shows MIP1α expressed in alveolar macrophages of lung tissue treated with saline (D), $anTiO_2$ (E) and $rnTiO_2$ (F). *, *** represent $p<0.05$ and 0.001, respectively, versus saline; ### represent $p<0.001$, versus $rnTiO_2$

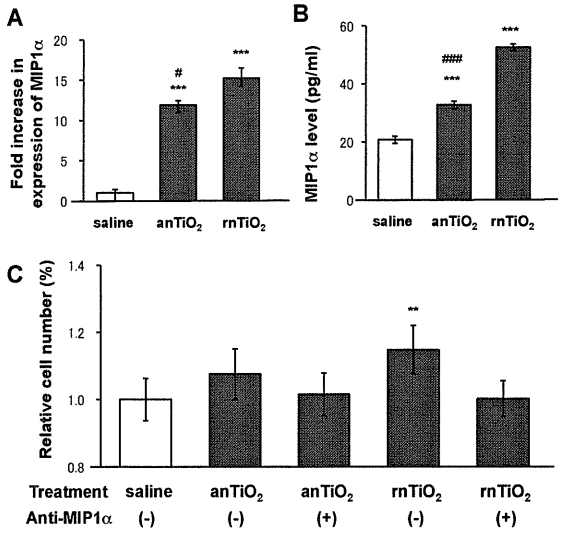

Figure 4. The Effect of $anTiO_2$ and $rnTiO_2$ on PAM Cells. The expression of MIP1α mRNA in cultured PAM (A) and protein in the culture media (B) indicate that treatment with $anTiO_2$ or $rnTiO_2$ increased MIP1α expression in the PAM. Conditioned cell culture media of PAM treated with $rnTiO_2$, but not $anTiO_2$, had a significant effect on proliferation of A549 cells, and this promotion was attenuated by addition of 20 μg/ml MIP1α neutralizing antibody (C). **, ***represent $p<0.01$ and 0.001, versus saline; #, ###represent $p<0.05$ and 0.001, versus $rnTiO_2$

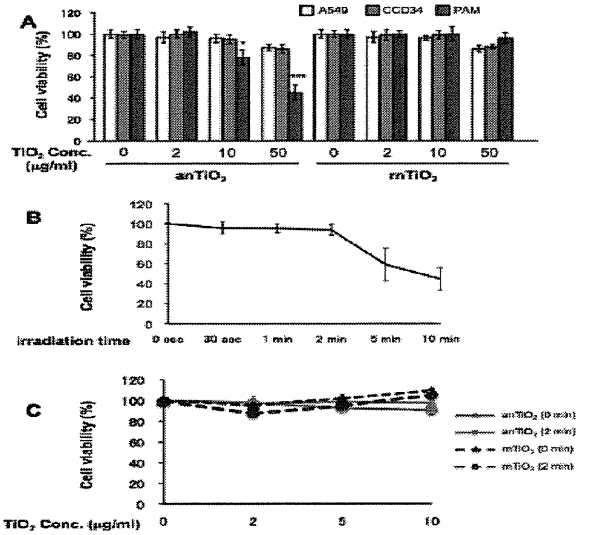

Figure 5. *In vitro* Assays. A: The effect of $anTiO_2$ and $rnTiO_2$ on the viability of A549, CCD34 and PAM cells. B: The effect of UVB irradiation on the viability of A549 cells. C: The effect of $anTiO_2$ and $rnTiO_2$ on the vi ability of A549 under UVB irradiation. *, *** represent $p<0.05$ and 0.001, versus the vehicle

(20.8±1.2 pg/mL). Both mRNA and protein expression of MIP1α was significantly lower in the $anTiO_2$ treated PAM compared to the $rnTiO_2$ treated cells.

The supernatants of the culture media of PAM treated with $anTiO_2$ showed only a tendency to increase A549 cell proliferation, while those collected from PAM treated with $rnTiO_2$ significantly promoted proliferation of A549 cells (115%) compared to supernatants from the saline treated group (Figure. 4C). The promotion effect of the supernatants of PAM cell cultures treated with $anTiO_2$or

rnTiO$_2$ was attenuated by anti-MIP1α neutralizing antibodies, indicating MIP1α is probably a mediator of the increase in A549 cell proliferation.

In vitro cytotoxicity assays

In vitro cytotoxicity assays indicated that both anTiO$_2$ and rnTiO$_2$ had little effect on the cell viability of A549 and CCD34 cells at a concentration of up to 50 mg/ml. anTiO$_2$ had a cytotoxic effect on the cell viability of PAM at doses of 10 and 50 mg/ml, while rnTiO$_2$ did not impair the cell viability of PAM at any of the examined concentrations (Figure. 5A).

To investigate whether UVB irradiation affected the cytotoxic effects of anTiO$_2$ and rnTiO$_2$ on cell viability, we first determined the exposure times that ultraviolet B irradiation itself did not impair the viability of A549 cells. As shown in Figure. 5B, irradiation for up to 2 min did not have any effect on the viability of A549 cells. With 2 min of UVB irradiation, neither anTiO$_2$ or rnTiO$_2$ at doses of 2, 5 or 10 μg/ml resulted in any decrease in the viability of A549 cells (Figure. 5C).

Discussion

The toxicity of nanoparticles usually includes tiers of biological responses such as induction of ROS and inflammation (Nel et al., 2006). This may contribute to carcinogenic potential (Tsuda et al., 2009). Thus, in the present study, we compared several parameters ofr inflammation and oxidative stress induced by TIPS of anTiO$_2$ and rnTiO$_2$. The results indicated that both anTiO$_2$ and rnTiO$_2$ particles were phagocytosed by alveolar macrophages and did not cause strong lung inflammation. Treatment with anTiO$_2$ and rnTiO$_2$ increased alveolar macrophage infiltration, MIP1α expression and 8-OHdG production: anTiO$_2$ had less effect than rnTiO$_2$.

Phagocytosis by alveolar macrophages is a major defense mechanism for deposition and clearance of inhaled particles (Heppleston, 1984; Rom et al., 1991; Geiser et al., 2008). However, activation of alveolar macrophages is strongly associated with inflammatory reactions and ROS production (Renwick et al., 2001; Bhatt et al., 2002; Wang et al., 2007). Also, MIP1α, secreted from rnTiO$_2$ burden alveolar macrophages, is possibly involved in the promotion of lung carcinogenesis (Xu et al., 2010). Similarly, pleural macrophage recruitment and activation are involved in the pathogenesis of asbestos (Choe et al., 1997). These results indicate two contrasting roles of alveolar macrophages in pathogenesis and host defense.

The toxic effects of nanoparticles are dependent on their size, shape, surface functionality and composition (Albanese et al., 2012). In the present study, we used comparable sizes of anTiO$_2$ and rnTiO$_2$ particles. Both types of nTiO$_2$ had no surface coating and had no obvious difference in elemental composition. Therefore, differences in alveolar macrophage induction, MIP1α expression and 8-OHdG production between anTiO$_2$ and rnTiO$_2$ are likely due to their different crystal structures and shapes. The lower toxicity of anTiO$_2$ compared to rnTiO$_2$ in the absence of UVB irradiation in our study is consistent with a previous *in vitro* study with bulk rutile and anatase TiO$_2$ (Gurr et al., 2005). In contrast to a previous study (Sayes et al., 2006), in the present study anTiO$_2$ and rnTiO$_2$ did not exhibit different toxicities on the cell viability of A549 cells under ultraviolet irradiation.

It should be noted that both types of anTiO$_2$ and rnTiO$_2$ particles formed aggregates in suspension, and aggregation may alter their bio-reactivity. Whether anTiO$_2$ and rnTiO$_2$ particles have different long-term effects remains to be clarified.

In conclusion, *in vivo* exposure of the rat lung to anTiO$_2$ or rnTiO$_2$ particles increased alveolar macrophage infiltration, MIP1α expression and 8-OHdG production, with anTiO$_2$ eliciting lower levels of biological responses than rnTiO$_2$. Similarly, exposure of primary alveolar macrophages to rnTiO$_2$ *in vitro* resulted the cells producing more MIP1α mRNA and protein than cells exposed to anTiO$_2$. Cytotoxicity assays *in vitro* indicated that both anTiO$_2$ and rnTiO$_2$ had very low cellular toxicity even under UVB irradiation.

Acknowledgements

This work was supported by Health and Labour Sciences Research Grants (Research on Risk of Chemical substance, H19-kagaku-ippan-006 and H22-kagaku-ippan-005). We thank Chisato Ukai and Takako Narita for their excellent secretarial assistance for the work.

References

Albanese A, Tang PS, Chan WC (2012). The effect of nanoparticle size, shape, and surface chemistry on biological systems. *Annu Rev Biomed Eng*, **14**, 1-16.

Bhatt NY, Kelley TW, Khramtsov VV, et al (2002). Macrophage-colony-stimulating factor-induced activation of extracellular-regulated kinase involves phosphatidylinositol 3-kinase and reactive oxygen species in human monocytes. *J Immunol*, **169**, 6427-34.

Choe N, Tanaka S, Xia W, et al (1997). Pleural macrophage recruitment and activation in asbestos-induced pleural injury. *Environ Health Perspect*, *105*, 1257-60.

Geiser M, Casaulta M, Kupferschmid B, et al (2008). The role of macrophages in the clearance of inhaled ultrafine titanium dioxide particles. *Am J Respir Cell Mol Biol*, **38**, 371-6.

Gurr JR, Wang AS, Chen CH, et al (2005). Ultrafine titanium dioxide particles in the absence of photoactivation can induce oxidative damage to human bronchial epithelial cells. *Toxicology*, **213**, 66-73.

Heppleston AG (1984). Pulmonary toxicology of silica, coal and asbestos. *Environ Health Perspect*, **55**, 111-27.

IARC (2010). Carbon black, titanium dioxide, and talc. *IARC Monogr Eval Carcinog Risks Hum*, **93**, 1-413.

Kakinoki K, Yamane K, Teraoka R, et al (2004). Effect of relative humidity on the photocatalytic activity of titanium dioxide and photostability of famotidine. *J Pharm Sci*, **93**, 582-9.

Maynard AD, Aitken RJ, Butz T, et al (2006). Safe handling of nanotechnology. *Nature*, **444**, 267-9.

Mohr U, Ernst H, Roller M, et al (2006). Pulmonary tumor types induced in Wistar rats of the so-called "19-dust study". *Exp Toxicol Pathol*, **58**, 13-20.

Nel A, Xia T, Madler L, et al (2006). Toxic potential of materials at the nanolevel. *Science*, **311**, 622-7.

Renwick LC, Donaldson K, Clouter A (2001). Impairment of alveolar macrophage phagocytosis by ultrafine particles.

Toxicol Appl Pharmacol, **172**, 119-27.

Rom WN, Travis WD, Brody AR (1991). Cellular and molecular basis of the asbestos-related diseases. *Am Rev Respir Dis*, **143**, 408-22.

Sayes CM, Wahi R, Kurian PA, et al (2006). Correlating nanoscale titania structure with toxicity: a cytotoxicity and inflammatory response study with human dermal fibroblasts and human lung epithelial cells. *Toxicol Sci*, **92**, 174-85.

Schulte P, Geraci C, Zumwalde R, et al (2008). Occupational risk management of engineered nanoparticles. *J Occup Environ Hyg*, **5**, 239-49.

Tsuda H, Xu J, Sakai Y, Futakuchi M, Fukamachi K (2009). Toxicology of engineered nanomaterials - A review of carcinogenic potential. *Asian Pac J Cancer Prev*, **10**, 975-980.

Wang H, Li J, Quan X, et al (2007). Formation of hydrogen peroxide and degradation of phenol in synergistic system of pulsed corona discharge combined with TiO_2 photocatalysis. *J Hazard Mater*, **141**, 336-43.

Wu J, Liu W, Xue C, et al (2009). Toxicity and penetration of TiO_2 nanoparticles in hairless mice and porcine skin after subchronic dermal exposure. *Toxicol Lett*, **191**, 1-8.

Xu J, Futakuchi M, Iigo M, et al (2010). Involvement of macrophage inflammatory protein 1alpha (MIP1alpha) in promotion of rat lung and mammary carcinogenic activity of nanoscale titanium dioxide particles administered by intrapulmonary spraying. *Carcinogenesis*, **31**, 927-35.

PLOS ONE

Rat N-ERC/Mesothelin as a Marker for *In Vivo* Screening of Drugs against Pancreas Cancer

Katsumi Fukamachi[1]*, Masaaki Iigo[2], Yoshiaki Hagiwara[3], Koji Shibata[1,4], Mitsuru Futakuchi[1], David B. Alexander[2], Okio Hino[5], Masumi Suzui[1], Hiroyuki Tsuda[2]

1 Department of Molecular Toxicology, Nagoya City University Graduate School of Medical Sciences, Nagoya, Japan, **2** Nanotoxicology Project, Nagoya City University, Nagoya, Japan, **3** Immuno-Biological Laboratories, Fujioka-shi, Gunma, Japan, **4** Division of Surgical Oncology, Department of Surgery, Nagoya University Graduate School of Medicine, Nagoya, Japan, **5** Department of Pathology and Oncology, Juntendo University School of Medicine, Tokyo, Japan

Abstract

Pancreatic ductal adenocarcinoma (PDA) is a highly lethal disease, which is usually diagnosed in an advanced stage. We have established transgenic rats carrying a mutated K-*ras* gene controlled by Cre/loxP activation. The animals develop PDA which is histopathologically similar to that in humans. Previously, we reported that serum levels of N-ERC/mesothelin were significantly higher in rats bearing PDA than in controls. In the present study, to determine whether serum levels of N-ERC/mesothelin correlated with tumor size, we measured N-ERC/mesothelin levels in rats bearing PDA. Increased serum levels of N-ERC/mesothelin correlated with increased tumor size. This result indicates an interrelationship between the serum level of N-ERC/mesothelin and tumor size. We next investigated the effect of chemotherapy on serum N-ERC/mesothelin levels. Rat pancreatic cancer cells were implanted subcutaneously into the flank of NOD-SCID mice. In the mice treated with 200 mg/kg gemcitabine, tumor weight and the serum level of N-ERC/mesothelin were significantly decreased compared to controls. These results suggest that serum N-ERC/mesothelin measurements might be useful for monitoring response to therapy.

Citation: Fukamachi K, Iigo M, Hagiwara Y, Shibata K, Futakuchi M, et al. (2014) Rat N-ERC/Mesothelin as a Marker for *In Vivo* Screening of Drugs against Pancreas Cancer. PLoS ONE 9(10): e111481. doi:10.1371/journal.pone.0111481

Editor: Mohammad Saleem, Hormel Institute, University of Minnesota, United States of America

Received June 2, 2014; **Accepted** September 25, 2014; **Published** October 27, 2014

Data Availability: The authors confirm that all data underlying the findings are fully available without restriction. All relevant data are within the paper and its Supporting Information files.

Funding: This work was supported in part by Adaptable and Seamless Technology transfer Program through target-driven R&D (A-STEP) from Japan Science and Technology Agency; a Grant-in-Aid for Scientific Research (C) from Japan Society for the Promotion of Science; a Grant-in-Aid for Research in Nagoya City University; the Aichi Cancer Research Foundation; the Program for developing the supporting system for upgrading the education and research from the Ministry of Education, Culture, Sports, Science and Technology; and a Grant-in-Aid for Cancer Research (17S-6, 20S-8) from the Ministry of Health, Labour and Welfare. The funders had no role in study design, data collection and analysis, decision to publish, or preparation of the manuscript.

Competing Interests: Yoshiaki Hagiwara is an employee of Immuno-Biological Laboratories. This does not alter the authors' adherence to all the PLOS ONE policies on sharing data and materials. The remaining authors declare no competing financial interests.

* Email: kfukamac@med.nagoya-cu.ac.jp

Introduction

N-ERC/mesothelin is a 31-kDa protein that forms the N-terminal fragment of the full-length 71-kDa ERC/mesothelin protein and is secreted into the blood of mesothelioma patients [1–3]. The rat *Erc* (expressed in renal cell carcinoma) gene was identified as a highly expressed gene in renal cell carcinoma of the Eker rat [4,5]. The human homolog of rat *Erc* is the *Mesothelin/megakaryocyte potentiating factor* (*MPF*) gene [6–8]. ERC/mesothelin is also expressed in ovary and pancreas carcinoma tissue in humans [9–12]. N-ERC/mesothelin is considered to be relevant in monitoring chemotherapeutic response in patients with mesothelioma [13,14].

Pancreatic ductal adenocarcinoma (PDA) carries the most dismal prognosis of all solid tumors [15]. We have established transgenic rat lines carrying a human $Hras^{G12V}$ (Hras250) [16] or a human $Kras^{G12V}$ (Kras301, Kras327) [17] oncogene in which the expression of the transgene is regulated by the Cre/loxP system. Targeted activation of the transgene is accomplished by injection of a Cre recombinase-carrying adenovirus (AxCANCre) into the pancreatic ducts through the common bile duct. Neoplastic lesions in the transgenic rats exhibit morphological [16,18] and biological [17,19–21] similarities to those observed in human pancreas lesions. We previously reported that N-ERC/mesothelin is readily detected in the serum of rats bearing pancreas ductal adenocarcinomas [17]. In the present study we report the use of N-ERC/mesothelin as a serum marker for evaluation of the effectiveness of chemotherapy.

Materials and Methods

Animals

Male $Kras^{G12V}$ transgenic (Kras301) rats (Jcl:SD rat background) were established as previously reported [17,18]. Homozygous rats were generated by breeding heterozygous male rats with heterozygous female rats. Homozygous transgenic rats were identified by semi-quantitative PCR and then confirmed by genetic testing. Kras301 rats were bred to obtain viable and fertile homozygous transgenic progeny. Fisher344 (F344/DuCrlCrlj) rats were purchased from Charles River Japan, Inc. (Yokohama, Japan). Sprague-Dawley (SD) rats (Jcl:SD) were obtained from CLEA Japan (Tokyo, Japan). SD (Slc:SD) and Wistar (Slc:Wistar/ST) rats were obtained from Japan SLC, Inc. (Hamamatsu, Japan). The rats were maintained in plastic cages in an air-

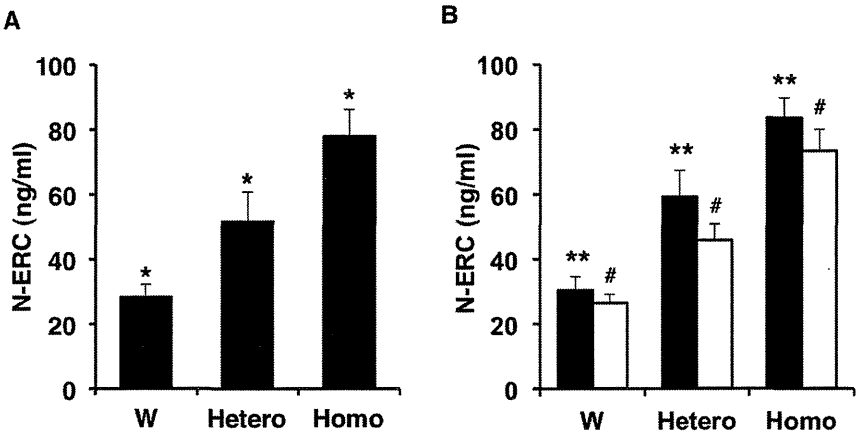

Figure 1. Comparison of serum levels of N-ERC/mesothelin in wild type Jcl:SD (W) and heterozygous (Hetero) and homozygous (Homo) Kras301 rats. Heterozygous Kras301 rats were generated by breeding homozygous Kras301 rats with wild type Jcl:SD rats. (A) Serum levels of N-ERC/mesothelin in wild type Jcl:SD rats and heterozygous and homozygous Kras301 rats. (B) Serum levels of N-ERC/mesothelin in male (closed bar) and female (open bar) wild type Jcl:SD rats and heterozygous and homozygous Kras301 rats. *, ** and #, P<0.0001 compared with each other.
doi:10.1371/journal.pone.0111481.g001

conditioned room with a 12-h light/12-h dark cycle. All experiments were conducted according to the Guidelines for Animal Experiments of the Nagoya City University Graduate School of Medical Sciences, and approved by the Animal Care and Use Committee of the Nagoya City University Graduate School of Medical Sciences (H21-02, H22M-24).

Tumor induction and pathological examination

Cre-expressing adenovirus vectors were amplified in HEK293 cells and then purified using Vivapure Adenopack (Vivascience, Hannover, Germany) as previously reported [17]. Pancreas tumors were induced as described previously [16–22]. The pancreas was fixed in 4% paraformaldehyde and processed for histological observation. Anti-rat C-ERC/mesothelin (306) was purchased from Immuno-Biological Laboratories (Gunma, Japan), and staining was performed as described previously [17].

Transplantation of a rat pancreas cell line and treatment with gemcitabine

A pancreas carcinoma cell line (634NOD) was established from a pancreas tumor from an Hras250 rat [17,23]. 634NOD tumor cells (2×10^6) were transplanted subcutaneously into 6 week old male NOD-SCID mice (CLEA Japan, Tokyo, Japan). One week later, NOD-SCID mice received gemcitabine (2′, 2′-difluoro deoxycytidine; dFdC) hydrochroride (Eli Lilly Japan K.K., Kobe, Japan) in saline four times within nine days by intraperitoneal injection. Tumors were measured by length (a) and width (b) in millimeters using calipers, and tumor volumes (V) were calculated according to the relationship $V = ab^2/2$, where "a" was the longer of the two measurements [24]. Seven weeks after transplantation, the mice were killed under deep isoflurane anesthesia and the tumors were removed and weighed and serum was collected for analysis of N-ERC/mesothelin.

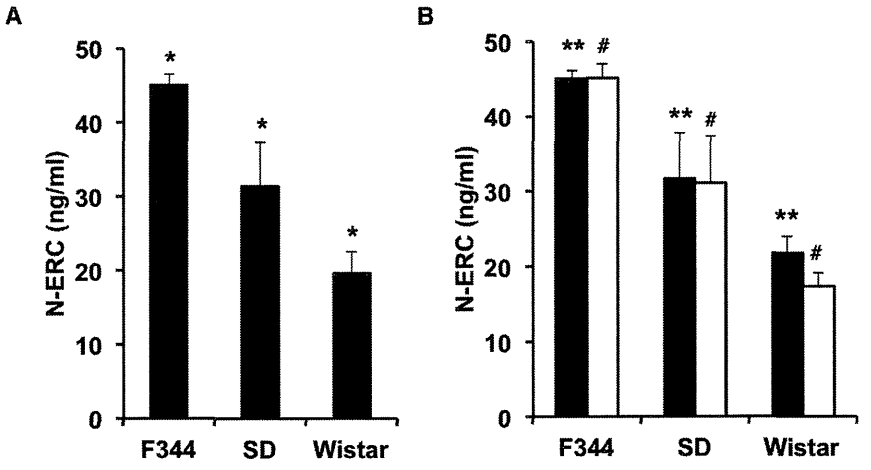

Figure 2. Comparison of serum levels of N-ERC/mesothelin in F344/DuCrlCrlj (F344), Slc:SD (SD) and Slc:Wistar/ST (Wistar) rat strains. (A) Strain differences in the serum levels of N-ERC/mesothelin. (B) Serum levels of N-ERC/mesothelin in males (closed bar) and females (open bar) of the different rat strains. *, P<0.0001; **, P<0.005; #, P<0.0001 compared with each other.
doi:10.1371/journal.pone.0111481.g002

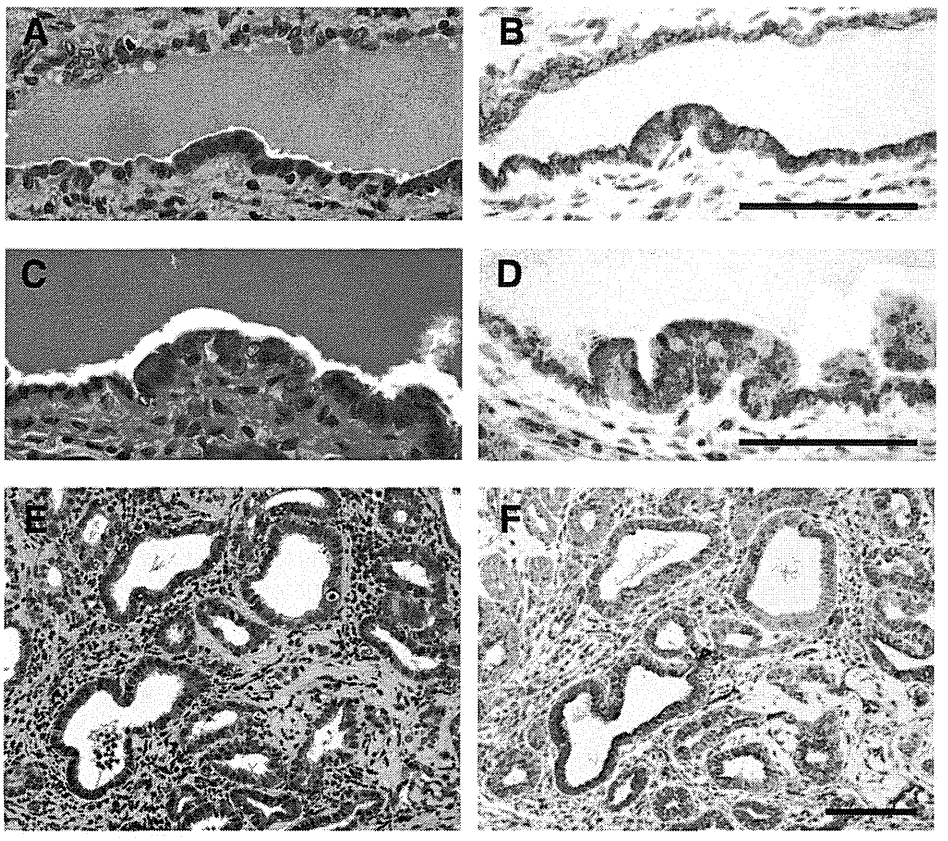

Figure 3. Expression of ERC/mesothelin in pancreatic lesions. Immunostaining of ERC/mesothelin in PanIN1 (A and B), PanIN2 (C and D) and PDA (E and F) lesions. A, C, E, H&E staining; B, D, F, ERC/mesothelin staining. Bars = 100 μm.
doi:10.1371/journal.pone.0111481.g003

Serum test

The serum level of rat N-ERC/mesothelin was quantified by ELISA (Code No.27765, Rat N-ERC/mesothelin Assay Kit, IBL, Gunma, Japan) as described previously [25].

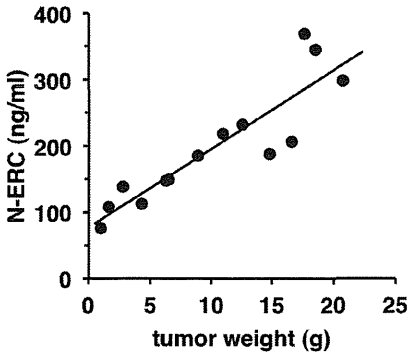

Figure 4. Correlation between tumor weight and serum level of N-ERC/mesothelin. The serum level of N-ERC/mesothelin in homozygous Kras301 rats bearing pancreas ductal carcinomas. The serum level of N-ERC/mesothelin correlated with increased tumor weight (R = 0.897).
doi:10.1371/journal.pone.0111481.g004

Results

Serum level of N-ERC/mesothelin in Kras301 rats

To determine whether the serum level of N-ERC/mesothelin is different in wild type Jcl:SD rats and heterozygous and homozygous Kras301 rats, we assayed N-ERC/mesothelin levels in wild type Jcl:SD rats and heterozygous and homozygous Kras301 rats at the age of 10 weeks: heterozygous F1 rats were generated by breeding homozygous male Kras301 rats with female Jcl:SD rats. There was no significant difference in body weight among the males or the females of the different genotypes (data not shown). The serum levels of N-ERC/mesothelin was significantly different between the three genotypes ($P<0.0001$): 28.3±4.0 ng/ml (n = 19) in the wild type Jcl:SD rats, 51.5±9.2 ng/ml (n = 19) in the heterozygous Kras301 rats, and 77.9±8.2 ng/ml (n = 13) in the homozygous Kras301 rats (Figure 1A). Furthermore, the serum level of N-ERC/mesothelin in heterozygous F1 rats was clearly higher than the original heterozygous rats [17].

There was no significant difference in serum N-ERC/mesothelin levels between male (30.3±4.2 ng/ml, n = 9) and female (26.4±2.8 ng/ml, n = 10) wild type Jcl:SD rats. In contrast, there was a significant difference in the serum levels of N-ERC/mesothelin between male and female heterozygous Kras301 F1 rats (male, 59.2±8.0 ng/ml, n = 8; female, 45.9±5.0 ng/ml, n = 11: $P<0.0001$) and homozygous Kras301 rats (male, 83.4±6.2 ng/ml, n = 6; female, 73.2±6.7 ng/ml, n = 7: $P<0.05$) (Figure 1B).

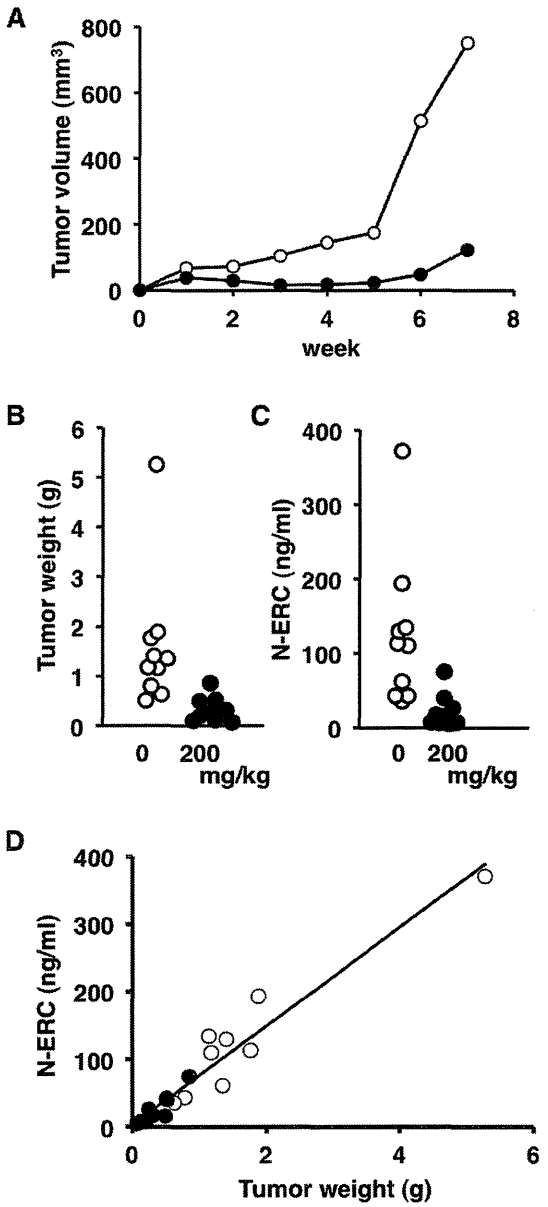

Figure 5. Effect of gemcitabine in NOD-SCID mice with transplanted 634NOD cells. Rat pancreas cancer cells (634NOD cells) were implanted subcutaneously into the flank of NOD-SCID mice. After 1 week the mice were administered gemcitabine (0 or 200 mg/kg, i.p.) four times within nine days by intraperitoneal injection. (A) Periodic observation of tumors in NOD-SCID mice treated with gemcitabine (0 mg/kg, open circles; 200 mg/kg, closed circles). (B) The tumor weight and (C) serum level of N-ERC/mesothelin was significantly decreased by treatment with gemcitabine (200 mg/kg, closed circles) compared to control (open circles) ($P<0.05$, $P<0.01$ respectively). (D) Correlation of tumor weight and serum levels of N-ERC/mesothelin. The serum level of N-ERC/mesothelin correlated with tumor weight and gemcitabine treatment ($R=0.966$). Open circles, 0 mg/kg; closed circles, 200 mg/kg. doi:10.1371/journal.pone.0111481.g005

Serum level of N-ERC/mesothelin in different rat strains

To determine whether the genetic background affected the serum levels of N-ERC/mesothelin, the levels of N-ERC/mesothelin in the serum were measured in three different rat strains: F344/DuCrlCrlj, Slc:Wistar/ST, and Slc:SD. The levels of N-ERC/mesothelin were significantly different between rat strains ($P<0.0001$) (Figure 2A). The levels of N-ERC/mesothelin were 45.0 ± 1.5 ($n=12$) in F344/DuCrlCrlj, 31.4 ± 5.9 ($n=12$) in Slc:SD and 19.6 ± 3.0 ($n=12$) in Slc:Wistar/ST rats. The levels of N-ERC/mesothelin were also significantly different between the males of the different strains and the females of the different strains (Figure 2B). In the individual strains, there was no significant difference between male ($n=6$) and female ($n=6$) rats (Figure 2B). Furthermore there was no significant difference between Jcl:SD ($n=19$) and Slc:SD ($n=12$) rats.

Serum level of N-ERC/mesothelin correlated with tumor size in rats

To determine whether serum levels of N-ERC/mesothelin correlated with tumor size, we assayed N-ERC/mesothelin levels in homozygous Kras301 rats bearing pancreas ductal adenocarcinomas. Adult male homozygous Kras301 rats were killed 4 weeks after injection of recombinant AxCANCre into the pancreatic duct via the common bile duct: see Fukamachi et al. 2013 [22] for a detailed description of AxCANCre-mediated activation of the Kras oncogene in Kras301 rats. Many grossly visible whitish tumor nodules were observed throughout the pancreas in the transgenic rats. Histological examination showed that these nodules were adenocarcinomas, as has been reported previously [16,17]. Neoplastic lesions were not found in any other organs. Immunohistochemical studies showed higher expression of ERC/mesothelin in carcinoma lesions compared to surrounding normal tissue, as has been reported previously [17]. Furthermore, immunohistochemical studies showed ERC/mesothelin was also positively expressed in pancreatic intraepithelial neoplasia (PanIN) lesions (Figure 3).

An increase in the serum level of N-ERC/mesothelin correlated with increased tumor size ($R=0.89665$, $P<0.0001$, $n=14$) (Figure 4). This result indicates an interrelationship between the serum level of N-ERC/mesothelin and tumor size in these rats.

N-ERC/mesothelin as a marker of the chemotherapeutic effect of an anti-cancer drug

We next investigated whether serum N-ERC/mesothelin levels were affected by treatment of pancreas adenocarcinoma with the chemotherapeutic drug gemcitabine. 634NOD cells [17], which were derived from a pancreas ductal adenocarcinoma from an Hras250 rat, were implanted subcutaneously into the flank of NOD-SCID mice. After 1 week the mice were administered gemcitabine (200 mg/kg, i.p.) four times within nine days by intraperitoneal injection. From week 1 to week 7 the tumor size continued to increase in both the control and the gemcitabine treated mice (Figure 5A). Although, due to the wide dispersion of tumor sizes, there was not a significant difference in tumor size between the two groups, the average tumor size was markedly smaller in the gemcitabine-treated mice compared to the control mice from week 3 to week 7 (Figure 5A). At the end of week 7, the mice were sacrificed and the tumors removed and weighed; the tumor weight in the gemcitabine-treated mice (0.33 ± 0.26 g, $n=9$) was significantly decreased compared to the control mice (1.60 ± 1.37 g, $n=10$) ($P<0.05$) (Figure 5B). There was no morphological difference between tumors from the gemcitabine-treated and control mice (data not shown). At the end of week 7, the serum level of N-ERC/mesothelin was significantly decreased ($P<0.01$) in mice treated with gemcitabine (22.4 ± 22.6 ng/ml, $n=9$) compared to the control mice (123.7 ± 100.6 ng/ml, $n=10$) (Figure 5C). In contrast, neither tumor weight nor serum levels of N-ERC/mesothelin were significantly different from the control ($n=10$) in mice treated with 75 ($n=10$) or 150 ($n=9$) mg/kg

gemcitabine (Figure S1). Although due to the wide dispersion of tumor sizes and N-ERC/mesothelin levels, there was not a significant difference in tumor size or N-ERC/mesothelin levels between the mice treated with 75 or 150 mg/kg gemcitabine and the control mice, the average of both values was smaller in the gemcitabine-treated mice compared to the control mice. Thus, the level of serum N-ERC/mesothelin correlated well with the effect of gemcitabine ($R = 0.96597$, $P<0.0001$) (Figure 5D).

Discussion

We have previously reported that the serum level of N-ERC/mesothelin correlated with tumor size in mice with transplanted rat pancreas cancer cells (634NOD cells) [17]. In the present study, in agreement with our previous report, the serum level of N-ERC/mesothelin correlated with pancreas tumor size in rats (Figure 4). These results showed that relative pancreas tumor size could be estimated from the serum level of N-ERC/mesothelin without sacrificing the animals. We also showed that N-ERC/mesothelin in the serum was a biomarker that could be used for monitoring the response to chemotherapy. When mice with tumors derived from transplanted 634NOD cells were treated with gemcitabine, tumor weight and the level of N-ERC/mesothelin in the serum were decreased compared with control. The serum level of N-ERC/mesothelin correlated with the therapeutic effect of the anti-cancer drug (Figure 5). Therefore, N-ERC/mesothelin can be used for quantitative analysis of the therapeutic effect of anti-cancer agents on pancreas cancer in the animal models used in this study.

The serum level of N-ERC/mesothelin in homozygous Kras301 rats was significantly higher than those of wild type rats. The serum level of N-ERC/mesothelin in heterozygous F1 of homozygous rats was also significantly higher than in wild type rats. However, the serum level of N-ERC/mesothelin in the original heterozygous rats were not different from wild type Jcl:SD rats [17]. The homozygous Kras301 rats were maintained by breeding homozygous male and homozygous female rats. It is likely that rats with high levels of N-ERC/mesothelin were accidentally selected in the course of establishing the homozygous Kras301 rats.

The serum level of N-ERC/mesothelin was significantly different among rat strains (F344/DuCrlCrlj, Slc:SD and Slc:Wistar/ST). These results suggest that the genetic background of different rat strains affects the basal level of serum N-ERC/mesothelin. Therefore, for the evaluation of chemotherapeutic responses using serum N-ERC/mesothelin, it is important to use appropriate controls.

N-ERC/mesothelin was detected in the supernatants of cultured human pancreas cancer cells and correlated with the expression levels of ERC/mesothelin [26]. ERC/mesothelin is frequently expressed in ductal carcinoma, but not in normal pancreas [11,26–28]. Thus, ERC/mesothelin expression can be found in both human and rat pancreas ductal adenocarcinoma. However, contrary to expectations, there was no significant difference in serum N-ERC/mesothelin concentrations between pancreas cancer patients and healthy control groups [26]. Therefore, while N-ERC/mesothelin can be used as a serum biomarker for pancreas ductal carcinoma in the animal models used in the present study, it is not suitable for humans.

Currently, there is no effective drug against pancreas cancer; therefore, the use of animal models to test the responsiveness of pancreas cancer to therapy remains of the utmost importance. The use of rat N-ERC/mesothelin as a serum marker lies in its ability to distinguish between rats with or without pancreas cancer without opening the abdominal cavity. Gemcitabine is generally considered to constitute first-line therapy for pancreatic cancer. The maximum tolerated dose of gemcitabine in rats was 50 mg/kg once a week. This dose had no effect on tumor size in Kras301 rats. Therefore, the serum level of N-ERC/mesothelin was not significantly affected in these animals (our unpublished results). Notably, in mice treated with gemcitabine, levels of gemcitabine that did not significantly affect tumor size did not affect the serum level of N-ERC/mesothelin (Figure S1). While gemcitabine alone does not show anti-cancer effects on endogenously developed pancreas cancer in rats (our unpublished result) or in mouse models [29], the results presented here demonstrate the usefulness of N-ERC/mesothelin as a serum marker in monitoring preclinical trials for therapy in mouse and rat models of pancreas ductal adenocarcinoma: serodiagnosis in animal models can be used to enhance screening for candidate chemotherapeutic agents that could be evaluated for human use.

Supporting Information

Figure S1 Effect of gemcitabine in NOD-SCID mice with transplanted 634NOD cells. The tumor weight and serum level of N-ERC/mesothelin was not decreased by treatment with 100 or 150 mg/kg gemcitabine.
(TIFF)

Author Contributions

Conceived and designed the experiments: KF MI HT. Performed the experiments: KF MI KS. Analyzed the data: KF MI MF MS HT. Contributed reagents/materials/analysis tools: KF YH OH HT. Contributed to the writing of the manuscript: KF DBA.

References

1. Shiomi K, Miyamoto H, Segawa T, Hagiwara Y, Ota A, et al. (2006) Novel ELISA system for detection of N-ERC/mesothelin in the sera of mesothelioma patients. Cancer Sci 97: 928–932.
2. Shiomi K, Hagiwara Y, Sonoue K, Segawa T, Miyashita K, et al. (2008) Sensitive and Specific New Enzyme-Linked Immunosorbent Assay for N-ERC/Mesothelin Increases its Potential as a Useful Serum Tumor Marker for Mesothelioma. Clin Cancer Res 14: 1431–1437.
3. Onda M, Nagata S, Ho M, Bera TK, Hassan R, et al. (2006) Megakaryocyte potentiation factor cleaved from mesothelin precursor is a useful tumor marker in the serum of patients with mesothelioma. Clin Cancer Res 12: 4225–4231.
4. Hino O, Kobayashi E, Nishizawa M, Kubo Y, Kobayashi T, et al. (1995) Renal carcinogenesis in the Eker rat. J Cancer Res Clin Oncol 121: 602–605.
5. Yamashita Y, Yokoyama M, Kobayashi E, Takai S, Hino O (2000) Mapping and determination of the cDNA sequence of the Erc gene preferentially expressed in renal cell carcinoma in the Tsc2 gene mutant (Eker) rat model. Biochem Biophys Res Commun 275: 134–140.
6. Chang K, Pastan I (1994) Molecular cloning and expression of a cDNA encoding a protein detected by the K1 antibody from an ovarian carcinoma (OVCAR-3) cell line. Int J Cancer 57: 90–97.
7. Chang K, Pastan I (1996) Molecular cloning of mesothelin, a differentiation antigen present on mesothelium, mesotheliomas, and ovarian cancers. Proc Natl Acad Sci U S A 93: 136–140.
8. Kojima T, Oh-eda M, Hattori K, Taniguchi Y, Tamura M, et al. (1995) Molecular cloning and expression of megakaryocyte potentiating factor cDNA. J Biol Chem 270: 21984–21990.
9. Scholler N, Fu N, Yang Y, Ye Z, Goodman GE, et al. (1999) Soluble member(s) of the mesothelin/megakaryocyte potentiating factor family are detectable in sera from patients with ovarian carcinoma. Proc Natl Acad Sci U S A 96: 11531–11536.
10. Hough CD, Sherman-Baust CA, Pizer ES, Montz FJ, Im DD, et al. (2000) Large-scale serial analysis of gene expression reveals genes differentially expressed in ovarian cancer. Cancer Res 60: 6281–6287.

11. Argani P, Iacobuzio-Donahue C, Ryu B, Rosty C, Goggins M, et al. (2001) Mesothelin is overexpressed in the vast majority of ductal adenocarcinomas of the pancreas: identification of a new pancreatic cancer marker by serial analysis of gene expression (SAGE). Clin Cancer Res 7: 3862–3868.
12. Saeki H, Hashizume A, Izumi H, Suzuki F, Ishi K, et al. (2012) The utility of serum N-ERC/mesothelin as a biomarker of ovarian carcinoma. Oncology letters 4: 637–641.
13. Tajima K, Hirama M, Shiomi K, Ishiwata T, Yoshioka M, et al. (2008) ERC/mesothelin as a marker for chemotherapeutic response in patients with mesothelioma. Anticancer research 28: 3933–3936.
14. Mori T, Tajima K, Hirama M, Sato T, Kido K, et al. (2013) The N-ERC index is a novel monitoring and prognostic marker for advanced malignant pleural mesothelioma. Journal of thoracic disease 5: 145–148.
15. Siegel R, Naishadham D, Jemal A (2012) Cancer statistics, 2012. CA: a cancer journal for clinicians 62: 10–29.
16. Ueda S, Fukamachi K, Matsuoka Y, Takasuka N, Takeshita F, et al. (2006) Ductal origin of pancreatic adenocarcinomas induced by conditional activation of a human Ha-ras oncogene in rat pancreas. Carcinogenesis 27: 2497–2510.
17. Fukamachi K, Tanaka H, Hagiwara Y, Ohara H, Joh T, et al. (2009) An animal model of preclinical diagnosis of pancreatic ductal adenocarcinomas. Biochem Biophys Res Commun 390: 636–641.
18. Tanaka H, Fukamachi K, Futakuchi M, Alexander DB, Long N, et al. (2010) Mature acinar cells are refractory to carcinoma development by targeted activation of Ras oncogene in adult rats. Cancer Sci 101: 341–346.
19. Yabushita S, Fukamachi K, Kikuchi F, Ozaki M, Miyata K, et al. (2013) Twenty-One Proteins Up-Regulated in Human H-ras Oncogene Transgenic Rat Pancreas Cancers are Up-Regulated in Human Pancreas Cancer. Pancreas 42: 1034–1039.
20. Yabushita S, Fukamachi K, Tanaka H, Fukuda T, Sumida K, et al. (2013) Metabolomic and transcriptomic profiling of human K-ras oncogene transgenic rats with pancreatic ductal adenocarcinomas. Carcinogenesis 34: 1251–1259.
21. Yabushita S, Fukamachi K, Tanaka H, Sumida K, Deguchi Y, et al. (2012) Circulating microRNAs in serum of human K-ras oncogene transgenic rats with pancreatic ductal adenocarcinomas. Pancreas 41: 1013–1018.
22. Fukamachi K, Tanaka H, Sakai Y, Alexander DB, Futakuchi M, et al. (2013) A novel reporter rat strain that expresses LacZ upon Cre-mediated recombination. Genesis 51: 268–274.
23. Fujii S, Fukamachi K, Tsuda H, Ito K, Ito Y, et al. (2012) RAS oncogenic signal upregulates EZH2 in pancreatic cancer. Biochem Biophys Res Commun 417: 1074–1079.
24. Carlsson G, Gullberg B, Hafstrom L (1983) Estimation of liver tumor volume using different formulas - an experimental study in rats. J Cancer Res Clin Oncol 105: 20–23.
25. Hagiwara Y, Hamada Y, Kuwahara M, Maeda M, Segawa T, et al. (2008) Establishment of a novel specific ELISA system for rat N- and C-ERC/mesothelin. Rat ERC/mesothelin in the body fluids of mice bearing mesothelioma. Cancer Sci 99: 666–670.
26. Inami K, Kajino K, Abe M, Hagiwara Y, Maeda M, et al. (2008) Secretion of N-ERC/mesothelin and expression of C-ERC/mesothelin in human pancreatic ductal carcinoma. Oncol Rep 20: 1375–1380.
27. Hassan R, Laszik ZG, Lerner M, Raffeld M, Postier R, et al. (2005) Mesothelin is overexpressed in pancreaticobiliary adenocarcinomas but not in normal pancreas and chronic pancreatitis. Am J Clin Pathol 124: 838–845.
28. Ordonez NG (2003) Application of mesothelin immunostaining in tumor diagnosis. Am J Surg Pathol 27: 1418–1428.
29. Olive KP, Jacobetz MA, Davidson CJ, Gopinathan A, McIntyre D, et al. (2009) Inhibition of Hedgehog signaling enhances delivery of chemotherapy in a mouse model of pancreatic cancer. Science 324: 1457–1461.

Biometals (2014) 27:1017–1029
DOI 10.1007/s10534-014-9747-2

Inhibition of intestinal polyp growth by oral ingestion of bovine lactoferrin and immune cells in the large intestine

Masaaki Iigo · David B. Alexander · Jiegou Xu · Mitsuru Futakuchi · Masumi Suzui · Takahiro Kozu · Takayuki Akasu · Daizo Saito · Tadao Kakizoe · Koji Yamauchi · Fumiaki Abe · Mitsunori Takase · Kazunori Sekine · Hiroyuki Tsuda

Received: 27 February 2014 / Accepted: 28 April 2014 / Published online: 28 May 2014

Abstract Studies using animal models have demonstrated that ingestion of bovine lactoferrin (bLF) inhibits carcinogenesis in the colon and other organs of experimental animals. As a result of these studies, a blinded, randomized, controlled clinical trial was conducted in the National Cancer Center Hospital, Tokyo, Japan to determine whether ingestion of bLF had an effect on the growth of colorectal polyps in humans. Patients with colorectal polyps $\leq$5 mm diameter and likely to be adenomas ingested 0, 1.5, or 3.0 g bLF daily for 1 year. Ingestion of 3.0 g bLF suppressed the growth of colorectal polyps and increased the level of serum human lactoferrin in trial participants 63 years old or younger. The purpose of the present study was to investigate correlations between immune parameters and changes in polyp size. Trial participants with regressing polyps had increased NK cell activity, increased serum hLF levels (indicating increased neutrophil activity), and increased numbers of CD4+ cells in the polyps. These findings are consistent with a correlation between higher immune activity and suppression of colorectal polyps. In addition, participants with regressing polyps had lower numbers of PMNs and increased numbers of S100A8+ cells in the polyps, consistent with a correlation between lower inflammatory potential in the colon and suppression of colorectal polyps. Trial participants ingesting bLF had increased serum hLF levels, a possible increase in systemic NK cell activity, and increased numbers of CD4+ and CD161+ cells in the polyps. Taken together, our findings suggest that bLF suppressed colorectal polyps by enhancing immune responsiveness.

Keywords Ingestion of bovine lactoferrin · Immune function · Human intestine · Ancillary study of a human clinical trial

Trial registration University Hospital Medical Information Network Clinical Trials Registry (UMIN-CTR; http://www.umin.ac.jp/ctr/index.htm) Tokyo, Japan: Trial number C000000182.

M. Iigo · D. B. Alexander · J. Xu · H. Tsuda (✉)
Nanotoxicology Project, Nagoya City University, Nagoya, Japan
e-mail: htsuda@phar.nagoya-cu.ac.jp

D. B. Alexander
e-mail: dalexand@phar.nagoya-cu.ac.jp

M. Futakuchi · M. Suzui
Department of Molecular Toxicology, Nagoya City University Graduate School of Medical Sciences, Nagoya, Japan

T. Kozu · T. Akasu · D. Saito · T. Kakizoe
National Cancer Center Central Hospital (as of 2005), Tokyo, Japan

K. Yamauchi · F. Abe · M. Takase · K. Sekine
Morinaga Milk Industry Co., Ltd., Minatoku, Japan

Introduction

Lactoferrin (LF) is an approximately 80 kDa protein present at high levels in milk, tear film, and neutrophil granules and at moderate to high levels in upper airway and seminal fluids (reviewed in Alexander et al. 2012). Endogenous LF is an important component of the innate immune system and its primary role is the non-lethal, non-inflammatory removal of microbial pathogens from cells and tissues.

The activity of LF ingested by adults is distinct from the activity of endogenous LF (see Alexander et al. 2012): Ingestion of bovine lactoferrin (bLF) has been shown to induce the expression of cytokines in the intestine, enhance the activity of immune effector cells, and inhibit carcinogenesis in the colon and other organs of experimental animals (reviewed in Tsuda et al. 2010).

As a result of the studies demonstrating an inhibitory effect of ingested bLF on colon carcinogenesis, a randomized, controlled clinical trial beginning in 2002 and ending in 2006 was conducted in the National Cancer Center Hospital, Tokyo, Japan to determine whether ingestion of bLF had an effect on the growth of adenomatous colorectal polyps in humans (Kozu et al. 2009). Briefly, trial participants ingested 0, 1.5, or 3.0 g bLF daily for 1 year: The size of colorectal polyps was measured prior to the beginning and at the end of the trial; peripheral blood samples were collected at the commencement of the trial and at the end of 3, 6, 9, and 12 months (the end of the trial), and T cell subpopulation numbers, natural killer cell activity and number, neutrophil number, and the serum levels of interleukin-18, interferon-gamma, and human lactoferrin (hLF) were measured; normal mucosa, close to the polyp, was collected prior to the beginning and at the end of the trial and polyps were collected at the end of the trial for RNA extraction and histological examination. The trial reported that ingestion of 1.5 g bLF had no significant effect on any of the parameters measured. Ingestion of 3.0 g bLF, however, had two significant effects: (i) the growth of colorectal polyps was inhibited in trial participants 63 years old or younger and (ii) the level of hLF in the serum was increased in trial participants 63 years old or younger (Kozu et al. 2009). The authors of the Tokyo-trial concluded that ingestion of 3.0 g bLF daily for one year inhibited the growth of adenomatous colorectal polyps and probably acted via modulation of immune system function.

Studies with animal models that have shown ingestion of bLF promoted immune system activity agree with the conclusions drawn from the Tokyo-trial: bLF-mediated inhibition of colorectal polyp growth probably acted via modulation of immune system function. The present study was undertaken to determine if immune cell parameters in the Tokyo-trial participants could be correlated with the changes in colorectal polyp size observed in the trial.

Methods

The Tokyo trial

A blinded, randomized, controlled clinical trial beginning in 2002 and ending in 2006 was conducted in the National Cancer Center Hospital, Tokyo, Japan to determine if ingestion of bLF would inhibit the growth of precancerous, adenomatous colorectal polyps in human patients. A complete description of the Tokyo-trail design, participants, interventions, outcomes, sample size, randomization, blinding, statistical methods, characteristics of the intent-to-treat population at the commencement of the trial, and the CONSORT flowchart are presented in Kozu et al. (2009).

Ethics statement

The Tokyo-trial was initiated after approval by the Ethical Committee of the National Cancer Center Hospital, Tokyo, Japan and is registered in the University Hospital Medical Information Network Clinical Trials Registry (UMIN-CTR; http://www.umin.ac.jp/ctr/index.htm) Tokyo, Japan, number C000000182. All trial participants provided written informed consent.

NK activity in the blood

Peripheral blood was collected from participants at the beginning of the trial and at 3, 6, 9, and 12 months (at the end of the trial). Blood samples used to measure NK cell activity were diluted with saline, and lymphocytes were separated from the diluted blood samples using Ficoll-Conray solution (relative density, 1.077; IBL). The entire lymphocyte population (containing effector cells) was washed twice with PBS. Cell killing activity was then measured using

K-562 cells labeled with ^{51}Cr as target cells. Target cells (1×10^6/mL, 10 μL) and effector cells (1×106/mL, 200 μL) were mixed and incubated at 37 °C, 5 % CO_2 for 3.5 h. The medium was then removed and clarified by centrifugation, and soluble ^{51}Cr released by killed K- 562 cells was measured with a gamma-counter (1470 Wizard, Perkin- Elmer Life and Analytical Sciences).

ELISA for serum lactoferrin

Peripheral blood was collected from trial participants as noted above. Microtiter plates were coated with a mouse anti-hLF antibody (mouse, clone: 2B8, IgG1, Advanced Immuno Chemical) and incubated at 5 °C overnight. To block the wells, 250 μL of 0.5 % gelatin in PBS was added to the wells and the plate was incubated at 37 °C for 1 h. 100 μL of sample was applied to the blocked wells and the plate was incubated at 5 °C overnight. Captured hLF was detected using horseradish peroxidase–labeled polyclonal antibodies against hLF (rabbit; Cappel) and visualization was done using o-phenylenediamine (Sigma). The minimal detectable concentration of hLF was 200 pg/mL; the minimal detectable concentration of bLF (using the hLF ELISA) was >20 μg/mL. The ELISA for bLF, using a specific antibody against bLF developed by Morinaga Milk Industry, was done similarly. Briefly, microtiter plates were coated with capture antibody (anti-bLF rabbit polyclonal, Morinaga Milk Industry) and blocked, and 100 μL sample was applied. Captured bLF was detected using a biotin-labeled anti-bLF polyclonal antibody (rabbit; Nacalai, Japan) and visualized with horseradish peroxidase–labeled streptavidin (Zymed) and o-phenylenediamine. The minimal detectable concentration of bLF was 500 pg/mL; the minimal detectable concentration of hLF (using the bLF ELISA) was >20 μg/mL.

Collection of tissue samples

Target polyps and tissue sample sites were located at the most proximal sites of the right colon (cecum to transverse colon) and the left colon (descending colon to rectum). Prior to the start of the trial a small tissue sample was collected from normal mucosa close to the target polyp. At the end of the trial period, a final colonoscopic examination was performed and a second normal tissue sample was collected and target polyps (and all other premalignant and malignant growths found) removed. Afer collection, tissue and polyp samples were immediately transferred to the laboratory on ice and divided into halves; RNA was extracted from one half, and the other half was immediately fixed in buffered formalin, embedded in paraffin, and processed for histopathological examination.

Counting polymorphonuclear leukocytes in the target polyps

Sections stained with H&E were used to count PMNs. PMNs were counted in the stroma of adenomatous polyps. Only polyp sections containing at least 5 atypical adenoma glands and mucosa propria to a depth equal to at least the average gland diameter (d) were used. PMNs in the stroma of 5 glands and the underlying mucosa propria to depth "d" were counted. The area was measured using an image analysis system, Image Processor for Analytical Pathology (IPAP, Sumika Technos Corp., Osaka, Japan).

Immunohistochemistry

CD4+, CD161+, CD66b+, S100A8+, and S100A9+ cells were detected using anti-CD4 polyclonal antibody (A429, Rabbit polyclonal) diluted 1:125, anti-CD161 monoclonal antibody (abcam, Mouse monoclonal IgG2b) diluted 1:100, ant-CD66b monoclonal antibody (Bioleggend, Mouse IgM) diluted 1:125, anti-S100A8 monoclonal antibody (MAC 387, Gene Tex, Mouse monoclonal IgG1) diluted 1:500, and anti-S100A9 monoclonal antibody (EPR3555, Gene Tex, Rabbit monoclonal IgG) diluted 1:5000. Positive cells were visualized with secondary antibody and Vectastain elite ABC kit. Slides were prepared according to Leica microsystems protocol: DeWax 5 min, high temperature antigen unmasking, 5 % H_2O_2 5 min, blocking 5 min, first antibody 60 min, second antibody 30 min, DAB 30 min, hematoxylin 5 min.

Statistics

The data for NK activity in the blood and serum hLF levels was analyzed using Dunnett's test. The data for PMN cells in the polyps was analyzed using Dunnett's test. The data for markers expressed primarily by a

single cell type (CD66b, CD4 and CD161) was analyzed using Dunnett's test. The data for markers expressed primarily by multiple cell types (S100A8+ and S100A9+) was analyzed using Hsu's MCB test. Pearson coefficients of correlation were calculated to determine the degree of association between polyp size and immune cells in the polyp. Levels of significance were set at 0.05 (two-sided) for all statistical analyses.

Results and discussion

Correlation of immune parameters with polyp growth

Systemic NK cell activity and blood PMN counts and serum hLF

As previously reported by Kozu et al. (2009), for the Tokyo-trial participants there was a statistically significant correlation between polyp growth during the one-year trial period and systemic NK activity and between polyp growth and levels of serum hLF. Polyp size, NK activity, and hLF levels in peripheral blood samples were measured prior to the beginning and at the end of the trial. 19 participants had target polyps that had increased in size by 20 % or more (growing polyps), 11 participants had target polyps that had decreased in size by 20 % or more (regressing polyps), and the remaining 73 participants had polyps that were diagnosed as having no change in size. The relative change in NK activity in the blood of the trial participants at the end of the one-year trial period was significantly higher in participants with regressing polyps compared to participants with growing polyps (Fig. 1). The change in hLF levels in the blood of the trial participants at the end of the one-year trial period was also significantly higher in participants with regressing polyps compared to participants with growing polyps (Fig. 2). Importantly, the overall number of neutrophils in the serum was not increased in patients with regressing polyps (data not shown). Therefore, since serum hLF is derived primarily from neutrophils (Ambruso et al. 1984; Gessler et al. 2004; Lash et al. 1983; van der Strate et al. 1999; Brown et al. 1986, 1983), the increase in serum hLF levels suggest that in patients with regressing polyps, serum neutrophils were more active than serum neutrophils

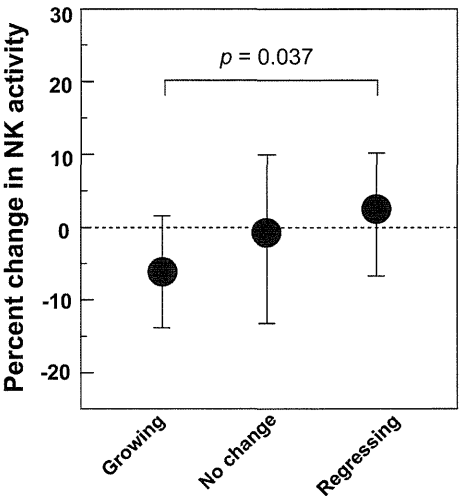

Fig. 1 Systemic NK cell activity and polyp growth. Polyp size and NK activity in peripheral blood samples were measured prior to the beginning and at the end of the trial. 19 participants had target polyps that had increased in size by 20 % or more (growing polyps), 11 participants had target polyps that had decreased in size by 20 % or more (regressing polyps), and the remaining 73 participants had polyps that were diagnosed as having no change in size. The relative change in NK activity in the blood of the trial participants at the end of the one-year trial period was significantly higher in participants with regressing polyps compared to participants with growing polyps. This figure is adapted from Fig. S2, Kozu et al. (2009), Effect of Orally Administered Bovine Lactoferrin on the Growth of Adenomatous Colorectal Polyps in a Randomized, Placebo-Controlled Clinical Trial

in participants with growing polys. Taken together, these data suggest that, on average, trial participants with regressing polyps had higher levels of immune system activity, as manifested by higher levels of systemic NK cell and neutrophil activity, than participants with growing polyps.

Polyp-associated CD4+ cells

There was a significant inverse correlation between the change in polyp size and the density of CD4+ cells in the polyp (Fig. 3a), and regressing polyps contained a significantly higher density of CD4+ cells than growing polyps (Fig. 3b). This is consistent with the key role helper T cells play in the immune system and suggests that activation of immune cells by helper T cells may play a role in inhibiting the growth of colorectal polyps. The increase of CD4+ cells in

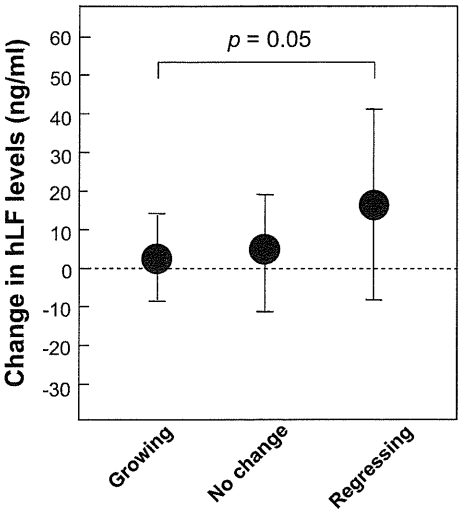

Fig. 2 Serum hLF levels and polyp growth. Polyp size and hLF levels in peripheral blood samples were measured prior to the beginning and at the end of the trial. 19 participants had target polyps that had increased in size by 20 % or more (growing polyps), 11 participants had target polyps that had decreased in size by 20 % or more (regressing polyps), and the remaining 73 participants had polyps that were diagnosed as having no change in size. The change in hLF levels in the blood of the trial participants at the end of the one-year trial period was significantly higher in participants with regressing polyps compared to participants with growing polyps

regressing polyps is consistent with the proposition stated above that, on average, participants with regressing polyps had higher levels of immune system activity than participants with growing polyps.

Polyp-associated CD161+ cells

CD161+ cells (primarily NK cells) were not increased in regressing polyps (data not shown). This result would appear to contravene the proposition that colorectal polyps were suppressed in trial participants with higher immune system activity. However, the most likely reason that NK cells were not increased in regressing polyps is that in general pre-cancerous polyp cells are essentially normal and are not targeted by the immune system. Therefore, immune cells involved in immunosurveillance and removal of transformed cells, such as NK cells, will be active in the polyps only sporadically, as pre-cancerous cells become transformed from pre-cancerous cells into cells with increased tumorigenic potential and become targets of the immune system. Consequently, even in patients with higher systemic NK cell activity, a sustained increase of NK cells in pre-cancerous colorectal polyps would not be expected to occur.

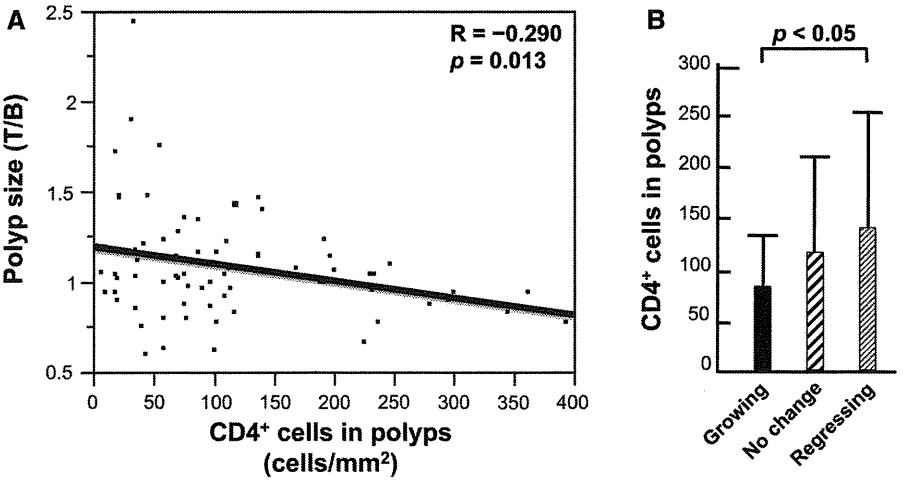

Fig. 3 Polyp-associated CD4+ cells and polyp growth. At the end of the trial, a final colonoscopic examination was performed. All target polyps were then removed and processed for histological examination. 91 polyps were histologically diagnosed, and the density of CD4+ cells could be determined by immunohistochemistry in 72 of these polyps: 28 target polyps had increased in size by 10 % or more (growing polyps), 16 target polyps had decreased in size by 10 % or more (regressing polyps), and the remaining 28 polyps were diagnosed as having no change in size. **a** There was a significant inverse correlation between the numbers of CD4+ cells in the polyps and the change in polyp size during the one-year trial period. **b** There was a significantly higher density of CD4+ cells in regressing polyps compared to growing polyps

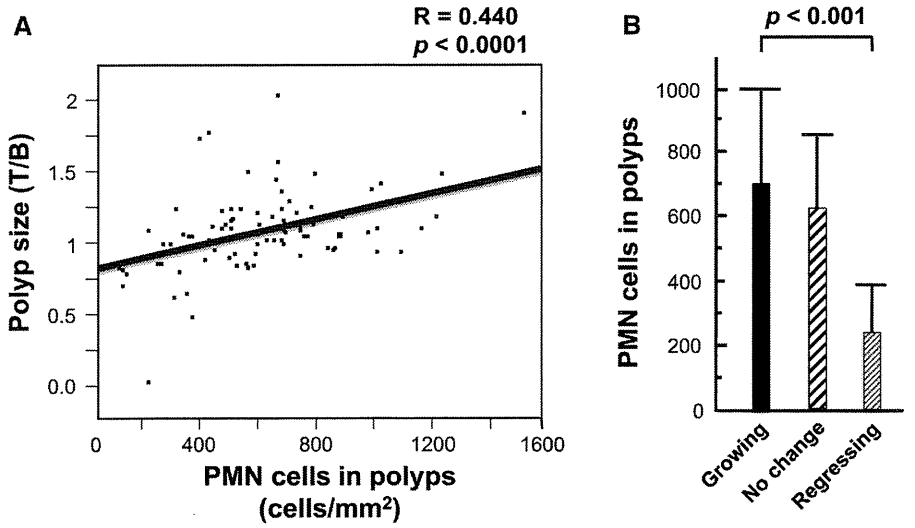

Fig. 4 Polyp-associated PMN leukocytes and polyp growth. At the end of the trial, a final colonoscopic examination was performed. All target polyps were then removed and processed for histological examination. 91 polyps were histologically diagnosed, and the density of PMNs in H&E stained sections could be determined in 88 of these polyps: 19 participants had target polyps that had increased in size by 20 % or more (growing polyps), 11 participants had target polyps that had decreased in size by 20 % or more (regressing polyps), and the remaining 58 participants had polyps that were diagnosed as having no change in size. **a** There was a significant correlation between polyp size and the numbers of PMN cells in the polyps. **b** There was a significantly higher density of PMN cells in growing polyps compared to regressing polyps. *Panel A* is adapted from Fig. 3, Kozu et al. (2009), Effect of Orally Administered Bovine Lactoferrin on the Growth of Adenomatous Colorectal Polyps in a Randomized, Placebo-Controlled Clinical Trial

Polyp-associated PMN leukocytes

As previously reported by Kozu et al. (2009), there was a significant correlation between polyp size and the density of PMNs in the polyp (Fig. 4a), and growing polyps contained a significantly higher density of PMNs than regressing polyps (Fig. 4b). While this result would also appear to contravene the proposition that colorectal polyps were suppressed, as manifested by their size and growth, in trial participants with higher immune system activity, three considerations demonstrate that the decrease of PMNs in regressing polyps is not at variance with this proposal. First, elevated immune system activity would encompass both immune cells that target transformed cells, such as NK cells, macrophages, and cytotoxic T cells, as well as immune cells that do not specifically target transformed cells such as PMNs. Therefore, elevated immune activity would not be expected to result in an increase of PMNs in regressing polyps. Second, as noted above, pre-cancerous polyp cells transform into cells with increased tumorigenic potential and become targets of the immune system only sporadically; therefore, signals that would induce PMN infiltration into the polyp (Bhatnagar et al. 2010) would be infrequent and brief. Third, infiltration of PMNs into a tumor site can enhance tumor growth (van den Tol et al. 2007; Wislez et al. 2007; Wada et al. 2007; Queen et al. 2005); therefore, decreased infiltration PMNs into colon polyps may partially account for the correlation between decreased polyp size and decreased PMN density in the polyp.

Polyp-associated CD66b+ cells

There was no correlation between polyp growth and the density of CD66b+ cells in the polyp (data not shown). CD66b is primarily expressed by activated granulocytes. This result indicates that activated granulocytes are not increased in regressing polyps and is consistent with the results obtained for activated NK cells: Signals that would activate granulocytes in the polyps, such as activated NK-mediated lysis of transformed cells (Bhatnagar et al. 2010), would be

present only transiently in the polyps, and therefore, a sustained increase of activated granulocytes would not be expected to occur in these polyps.

Polyp-associated S100A8+ and S100A9+ cells

Figure 5 shows typical S100A8+ cells (panel A) and S100A9+ cells (panel B). There was a significant inverse correlation between polyp size and the density of S100A8+ cells in the polyp (Fig. 6a), and there was an increase, although not significant, of S100A8+ cells in regressing polyps compared to growing polyps (Fig. 6b). There was no correlation between polyp-associated S100A9+ cells and polyp size or growth (data not shown). However, there was a significant inverse correlation between polyp size and the ratio of S100A8+/S100A9+ cells in the polyp (Fig. 7a), and the ratio of S100A8+/S100A9+ cells was significantly higher in regressing polyps than growing polyps (Fig. 7b). S100A8 and S100A9 heterodimerize to form calprotectin and are constitutively expressed at very high levels in neutrophils, in which calprotectin comprises over 40 % of the cytosolic proteins (Goyette and Geczy 2011). S100A8 and S100A9 are also constitutively expressed in myeloid-derived dendritic cells, osteoclasts, hypertrophic chondrocytes, and immature monocytes (Goyette and Geczy 2011). In addition, expression of either one or both of these proteins can be induced in microvascular endothelial cells, keratinocytes, and resident tissue macrophages (Goyette and Geczy 2011). The distribution of S100A8+ and S100A9+ in colorectal polyps is consistent with decreased infiltration of PMNs into regressing polyps and an accompanying increase of S100A8+ cells in these polyps. Human S100A8 and S100A9 are implicated in inflammation, however, the functions of human S100A8 and S100A9 are yet to be precisely defined (Goyette and Geczy 2011; Donato et al. 2013; Lim et al. 2009). In vitro studies with human S100A9 and in vivo studies with animal models indicate that S100A9 can have pro-inflammatory activity: Human S100A9 enhances neutrophil infiltration and retention in extra-vascular tissues (Schnekenburger et al. 2008; Anceriz et al. 2007; Newton and Hogg 1998) and promotes neutrophil degranulation (Simard et al. 2010) and phagocytosis (Simard et al. 2011). Murine S100A8 is also pro-inflammatory (Ryckman et al. 2003; Vandal et al. 2003). In contrast, human S100A8 is reported to have anti-inflammatory activity (Zhao et al. 2011; Lim et al. 2008; Hsu et al. 2005), mediated in part by inhibition of neutrophil infiltration and retention in extra-vascular tissues (Roth et al. 2003; Newton and Hogg 1998; Sroussi et al. 2006). The observation that the ratio of S100A8+/S100A9+ cells correlates with regressing polyps coupled with promotion of neutrophil infiltration by S100A9 and inhibition of neutrophil infiltration by S100A8 is consistent with the observed decrease of PMN infiltration in regressing polyps. The association of inflammation with carcinogenesis (Ichikawa et al. 2011; Gebhardt et al. 2006; Balkwill and Mantovani 2001) coupled with the pro-inflammatory activity of S100A9 and the anti-inflammatory activity of S100A8 is consistent with lower inflammatory potential and lower carcinogenic potential in regressing polyps.

Summary

Overall, our observations are consistent with the following paradigm. The colorectal polyps in patients with higher immune system activity had less growth potential, as manifested by their limited growth or regression during the one-year trial period, than polyps in patients with lower immune system activity. One likely mechanism by which the immune system acted was by eliminating polyp cells as they became transformed from pre-cancerous cells into cells with increased tumorigenic potential. In addition, the colorectal polyps in patients with lower inflammatory potential in their colon mucosa had less growth potential than the polyps in patients with greater inflammatory potential in their colon mucosa.

Effect of bLF on immune parameters

Systemic NK cell activity and blood PMN counts and serum hLF

There was an increase in NK activity in the serum of patients ingesting bLF, however, while the increase was statistically significant in participants ingesting 1.5 b bLF, the increase was not significant in participants ingesting 3.0 g bLF (Fig. 8). These incongruent results are consistent with a possible marginal increase in NK activity in participants ingesting bLF. There was also a statistically significant increase in the levels of serum hLF in trial participants

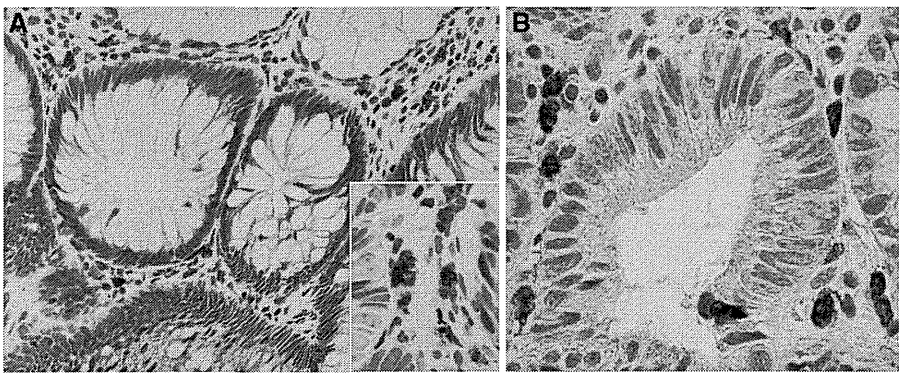

Fig. 5 S100A8+ and S100A9+ cells. Typical S100A8+ (**a**) and S100A9+ (**b**) cells in colorectal polyps are shown

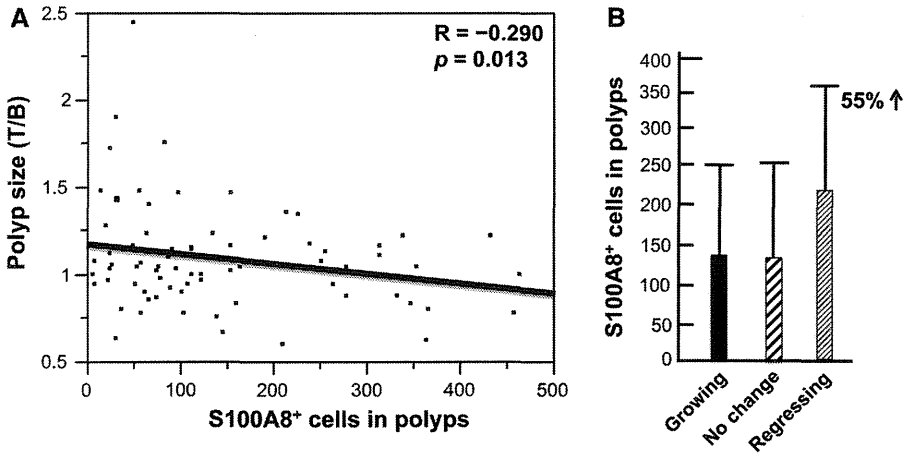

Fig. 6 Polyp-associated S100A8+ cells and polyp growth. At the end of the trial, a final colonoscopic examination was performed. All target polyps were then removed and processed for histological examination. 91 polyps were histologically diagnosed, and the density of S100A8+ cells could be determined by immunohistochemistry in 73 of these polyps: 29 participants had target polyps that had increased in size by 10 % or more (growing polyps), 16 participants had target polyps that had decreased in size by 10 % or more (regressing polyps), and the remaining 28 participants had polyps that were diagnosed as having no change in size. **a** There was a significant inverse correlation between polyp size and the numbers of S100A8+ cells in the polyps. **b** There was a non-significant increase in the density of S100A8+ cells in regressing polyps compared to growing polyps

ingesting 3.0 g bLF (Fig. 9). (bLF was not detected in the serum of any of the trial participants at any time.) In contrast to serum hLF levels, the increase in the number of PMNs in the blood of participants 63 years old and younger ingesting 3.0 g bLF was not significant (data not shown). As discussed above, since serum hLF is derived primarily from neutrophils (Ambruso et al. 1984; Gessler et al. 2004; Lash et al. 1983; van der Strate et al. 1999; Brown et al. 1986, 1983), the increase in serum hLF levels suggest that in these participants, serum neutrophils had elevated activity. Importantly, blood collection can provide an activating signal for primed neutrophils (Freitas et al. 2008) and as large amounts of lactoferrin are present in neutrophil granules, the presence of primed neutrophils in a blood sample will result in a measurable increase of lactoferrin in the serum obtained from that sample. The possible marginal increase in unstimulated NK cell activity and the significant increase in the activity of neutrophils stimulated by serum